Article

Immunity

Airway Epithelial Cell-Derived Colony Stimulating Factor-1 Promotes Allergen Sensitization

Graphical Abstract

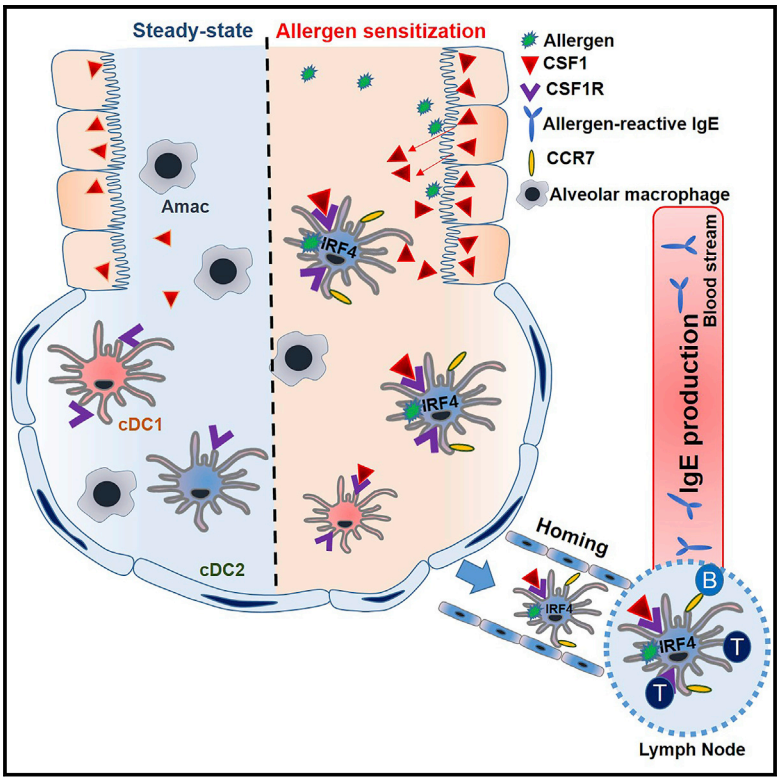

Authors

Hyung-Geun Moon, Seung-jae Kim, Jong Jin Jeong, ..., Steven J. Ackerman, John W. Christman, Gye Young Park

Correspondence

parkgy@uic.edu

In Brief

Airway epithelial cells are the first line of defense against foreign antigens and influence the microenvironment of the lung by secreting bioactive mediators. Moon and colleagues demonstrate that airway epithelial cells regulate dendritic cells for trafficking aeroallergen and subsequent development of adaptive immune responses.

Highlights

- Airway epithelial cells secrete CSF1 in response to aeroallergen challenge
- Epithelial-derived CSF1 is required for allergen-reactive IgE production
- CSF1R^{+} cDC2s are required for allergic inflammation
- CSF1-CSF1 receptor pathway regulates cDC2 migration to regional LNs

Moon et al., 2018, Immunity *49*, 1–13
August 21, 2018 © 2018 Elsevier Inc.
https://doi.org/10.1016/j.immuni.2018.06.009

CellPress

Please cite this article in press as: Moon et al., Airway Epithelial Cell-Derived Colony Stimulating Factor-1 Promotes Allergen Sensitization, Immunity (2018), https://doi.org/10.1016/j.immuni.2018.06.009

Immunity
Article

CellPress

Airway Epithelial Cell-Derived Colony Stimulating Factor-1 Promotes Allergen Sensitization

Hyung-Geun Moon,[1] Seung-jae Kim,[1] Jong Jin Jeong,[1,9] Seon-Sook Han,[1,10] Nizar N. Jarjour,[2] Hyun Lee,[3] Sherry L. Abboud-Werner,[4] Sangwoon Chung,[5] Hak Soo Choi,[6] Viswanathan Natarajan,[1,7] Steven J. Ackerman,[8] John W. Christman,[5] and Gye Young Park[1,11,*]

[1]Division of Pulmonary, Critical Care, Sleep and Allergy, Department of Medicine, University of Illinois at Chicago, Chicago, IL, USA
[2]Allergy, Pulmonary, and Critical Care Division, Department of Medicine, University of Wisconsin, Madison, WI, USA
[3]Center for Biomolecular Sciences, and Department of Medicinal Chemistry & Pharmacognosy, College of Pharmacy, University of Illinois at Chicago, Chicago, IL, USA
[4]Department of Pathology, University of Texas Health Science Center at San Antonio, San Antonio, TX, USA
[5]Section of Pulmonary, Critical Care, and Sleep Medicine, the Ohio State University, Davis Heart and Lung Research Center, Columbus, OH, USA
[6]Gordon Center for Medical Imaging, Division of Nuclear Medicine and Molecular Imaging, Massachusetts General Hospital, Boston, MA, USA
[7]Department of Pharmacology, University of Illinois at Chicago, Chicago, IL, USA
[8]Department of Biochemistry and Molecular Genetics, and Medicine, University of Illinois at Chicago, Chicago, IL, USA
[9]Present address: Section of Hematology/Oncology, Department of Medicine, University of Chicago, Chicago, IL, USA
[10]Present address: Department of Medicine, School of Medicine, Kangwon National University, Chuncheon, South Korea
[11]Lead Contact
*Correspondence: parkgy@uic.edu
https://doi.org/10.1016/j.immuni.2018.06.009

SUMMARY

Airway epithelial cells (AECs) secrete innate immune cytokines that regulate adaptive immune effector cells. In allergen-sensitized humans and mice, the airway and alveolar microenvironment is enriched with colony stimulating factor-1 (CSF1) in response to allergen exposure. In this study we found that AEC-derived CSF1 had a critical role in the production of allergen reactive-IgE production. Furthermore, spatiotemporally secreted CSF1 regulated the recruitment of alveolar dendritic cells (DCs) and enhanced the migration of conventional DC2s (cDC2s) to the draining lymph node in an interferon regulatory factor 4 (IRF4)-dependent manner. CSF1 selectively upregulated the expression of the chemokine receptor CCR7 on the CSF1R^{+} cDC2, but not the cDC1, population in response to allergen stimuli. Our data describe the functional specification of CSF1-dependent DC subsets that link the innate and adaptive immune responses in T helper 2 (Th2) cell-mediated allergic lung inflammation.

INTRODUCTION

The microenvironmental milieu determines the phenotype, function, and fate of immune cells. Airway epithelial cells (AECs) are the first line of defense against foreign antigens and influence the microenvironment of the lung by secreting bioactive mediators that can orchestrate the overall pulmonary immune response (Rivera et al., 2016; Whitsett and Alenghat, 2015). In asthma, AEC-derived cytokines (TSLP, IL-1α, and IL-33), chemokines (CCL2 and CCL20), and danger signals (ATP and uric acid) facilitate the recruitment of immune cells to inflamed regions and stimulate allergic inflammation (Whitsett and Alenghat, 2015). AECs are also known to regulate the activation and migration of lung DCs involved in the pathogenesis of asthma. It is known that toll-like receptor-4 (TLR4) activation of AECs is necessary for dendritic cell (DC) migration and subsequent development of asthma (Hammad et al., 2009), and primary human bronchial cells produce DC-attracting chemokines, granulocyte monocyte-colony stimulating factor (GM-CSF), and interleukin-33 (IL-33) in response to house dust mite (HDM) allergen (Willart et al., 2012).

Colony-stimulating factor-1 (CSF1), also known as macrophage-CSF (M-CSF), and its receptor (CSF1R), which is almost exclusively expressed by myeloid lineage cells, regulate the survival, proliferation, differentiation, and chemotaxis of tissue macrophages and dendritic cells, that play a key role in innate immune responses (Stanley and Chitu, 2014). The local concentration of CSF1 regulates DC and macrophage populations by inducing *in situ* proliferation and recruitment of their precursors into inflammatory and non-inflammatory conditions. In DCs, the CSF1R promoter is inactivated in DC precursors and is upregulated during differentiation (MacDonald et al., 2005), and CSF1 induces pre-DC extravasation into local tissues which regulates the magnitude of the tissue DC population (Guilliams and Scott, 2017; Tagliani et al., 2011). Furthermore, a genetic association between CSF1R polymorphism and a risk for asthma has been reported in humans (Shin et al., 2010).

Dendritic cells are the major antigen-presenting cells of the lung and play a crucial role in the immune response to inhaled allergen by taking up the antigen and transferring it to the mediastinal lymph nodes (mLNs) where they launch an antigen-specific adaptive immune response involving T and B cells (Joffre

et al., 2009). The transfer of allergen to the regional LNs occurs through active cellular transport by migratory DCs in a CCR7 chemokine receptor-dependent manner (Plantinga et al., 2013). Conventional DCs (cDCs) are described as classical antigen-presenting cell types of immune system and express higher CCR7 compared to other DC subsets (Worbs et al., 2017). Depletion of cDC in the lung abrogates the development of Th2 cell immunity and attenuates the hallmark features of asthma (Hammad et al., 2010). The various lung DC subsets play different roles in allergic lung inflammation. A recent study has shown that the DC subset, CD11b^{+} cDC2, is the more effective carrier of allergen to the regional LNs, compared to CD103^{+} cDC1s or monocyte-derived DCs (Plantinga et al., 2013). Upon primary sensitization to allergen delivered by migratory DCs, a low-intensity antigen-specific IgE response occurs. When re-challenged with allergen, there is an augmented secondary IgE response that is characteristic of a memory response (Talay et al., 2012). In particular, alveolar DCs are present in the bronchoalveolar lavage (BAL) fluid of non-diseased human lung (Desch et al., 2016; Patel et al., 2017) and their numbers are increased in human infants infected with respiratory syncytial virus (Kerrin et al., 2017), although their role is not well elucidated. Alveolar DCs are known to actively take up inhaled particles as they move through the alveolar spaces, and they traffic to regional LNs through a trans-epithelial migration process (Thornton et al., 2012).

Here, we demonstrated that spatiotemporally secreted CSF1 in the airways is necessary for regulating IgE production in response to allergen challenge in sensitized hosts. Our findings demonstrate that CSF1 secreted by airway epithelial cells (AECs) activates cDC2 trafficking to the draining LNs by enhancing CCR7 expression and promoting subsequent IgE production. These data provide a conceptual framework for understanding how the microenvironmental milieu has a critical role in bridging the innate and adaptive immune response in allergic lung inflammation.

RESULTS

Airway Epithelial Cells Secrete CSF1 into the Airspace in Response to Aeroallergen Challenge

We measured the CSF1 concentration in the bronchoalveolar lavage (BAL) fluids of patients with allergies and mild asthma who were enrolled in a subsegmental bronchoprovocation with allergen (SBP-AG) protocol as described previously (Park et al., 2013). Subjects with mild intermittent asthma and confirmed allergy to one of three IRB-approved aeroallergens (house dust mite, ragweed, or cockroach) underwent bronchoscopy with BAL twice, before and at 48 hr after SBP-AG. CSF1 was markedly increased in the post allergen challenge BAL fluid, whereas CSF2 (a.k.a. GM-CSF) remained unchanged (Figure 1A). These results were independently validated in another SBP-AG cohort analyzed from the University of Wisconsin at Madison (Figure 1B). CSF1 was secreted into the BAL fluid in a soluble form without packaging (Figure S1A); however, the plasma concentrations of CSF1 and CSF2 were not changed by SBP-AG (Figure S1B). Of note, the innate pro-Th2 cell cytokines, such as IL-33 and TSLP, were not changed in the BAL fluids by the allergen challenge in these cohorts, despite the fact that these cytokines are important for promoting Th2 cell immune responses at the epithelial basal layer (Figure S1C). We subjected mice to a combination house dust mite, ragweed, and *Aspergillus* allergen (DRA)-induced allergic asthma model, which is comparable to human SBP-AG, since DRA includes two of the allergens used for the human SBP-AG protocol as described previously (Park et al., 2013). The mouse model consists of an initial allergen sensitization followed by allergen challenge phase with three times of intranasal insufflation with DRA (Figure 1C). The DRA asthma model generated two peaks in serum IgE. The initial rise occurred in the sensitization phase and dropped to near baseline prior to re-challenge, followed by a massive secondary increase in serum IgE in response to allergen challenge in the sensitized mice (Figure S1D). The CSF1 concentrations in the DRA mouse asthma model peaked at an early time point of 6 hr after the last allergen challenge in both BAL fluids and lung lysates, whereas the CSF2 remained unchanged as seen in the human SBP-AG cohorts (Figure 1C). In contrast, CSF1 secretion was not induced in BAL fluids by *Pseudomonas aeruginosa*-induced lung infection, although CSF2 was increased at 6 and 24 hr (Figure 1D). Immunohistochemistry of lungs from mice subjected to the DRA asthma model showed a predominant expression of CSF1 in airway epithelial cells (AECs), indicating that AECs are the major site of CSF1 production in lung (Figure 1E). Similarly, BEAS-2B cells, a human bronchial epithelial cell line, secreted CSF1 upon DRA allergen challenge in a directional secretory pattern where CSF1 is secreted preferentially into the apical side rather than basal layer (Figure 1F).

Deletion of CSF1 in Airway Epithelial Cells Abolishes IgE Production and Subsequent Allergic Lung Inflammation

In order to block CSF1 activity in the airspaces, we utilized a neutralizing antibody of CSF1. Compared to mice subjected to isotype control IgG, mice inoculated by nasal insufflation with anti-CSF1 antibody had a marked reduction in eosinophil recruitment, production of Th2 cell cytokines, and allergic lung inflammation in the DRA asthma model in a dose-responsive manner (Figures 2A, S1E, and S1F). Of note, inhibition of CSF1 in the airspaces by the neutralizing antibody markedly lowered total and DRA-reactive of IgE (Figure 2B).

Airway epithelial cells recognize inhaled antigens and have an immunomodulatory role by secreting mediators (Hammad et al., 2009; Lambrecht and Hammad, 2012). To investigate the functional importance of CSF1 upregulation in the airway epithelium in asthma, we deleted *Csf1* selectively from airway epithelial cells by crossing a floxed *Csf1* mouse (*Csf1*$^{fl/fl}$) (Harris et al., 2012) with a *Scgb1a1-cre* mouse in which Cre recombinase is only expressed in AECs (*Scgb1a1-cre*ERT;*Csf1*$^{fl/fl}$). The injection of tamoxifen successfully blocked *Csf1* expression in the airway epithelium (Figure 2C). The mice were subjected to the DRA asthma model and tamoxifen injection (Tm_DRA) depleted CSF1 in BAL fluid and lung lysate (Figure 2D). Notably, the epithelial cell-specific *Csf1* deletion abolished the characteristics of allergic lung inflammation including eosinophil recruitment and increased Th2 cell cytokines, IL-4 and IL-13, in BAL fluids (Figures 2E–2G). The expression of total and DRA-reactive serum IgE was completely blocked in the tamoxifen-injected *Scgb1a1-cre*ERT;*Csf1*$^{fl/fl}$ mice, compared to mice injected by

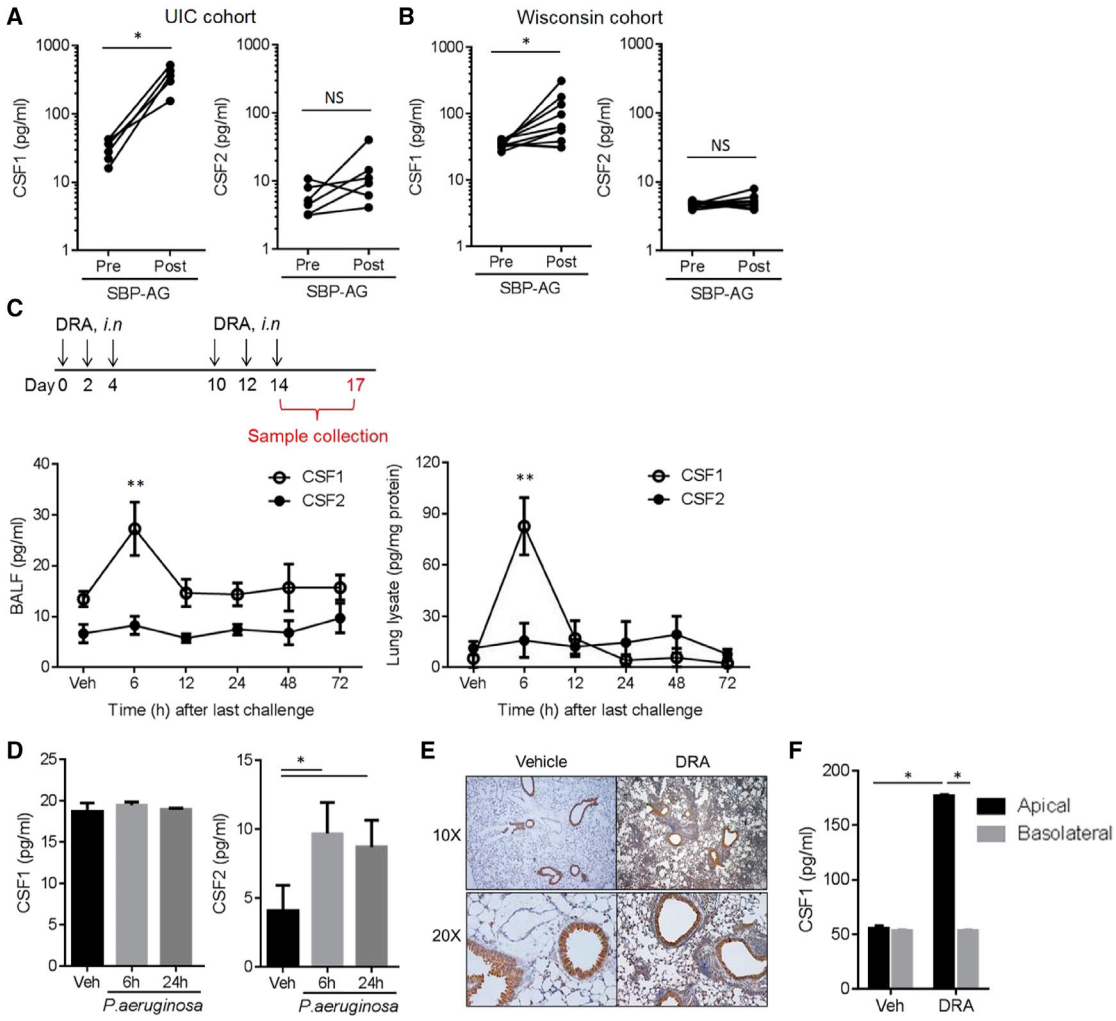

Figure 1. Airway Epithelial Cells Secrete CSF1 into the Airspace in Response to Aeroallergen Challenge

(A) CSF1 and CSF2 in BAL fluids obtained from patients with mild asthma enrolled in the UIC SBP-AG cohort (n = 6).

(B) CSF1 and CSF2 in the Wisconsin SBP-AG cohort (n = 10).

(C) Schematic of the DRA-induced mouse asthma model. DRA allergens were given intranasally (i.n.). CSF1 and CSF2 in BAL fluids (left) and lung lysates (right) in the DRA model (n = 5).

(D) Concentrations of BAL CSF1 and CSF2 in *P. aeruginosa* lung infection model (n = 3).

(E) Anti-CSF1 immunohistochemical (IHC) staining with lung tissues from the mice with DRA or vehicle only.

(F) CSF1 in the transwell media of primary bronchial epithelial cells (BEAS-2B) stimulated with DRA allergens (each 1 μg/mL) for 24 hr. The media from apical and basal chambers were independently collected.

Data represent at least two (C–E) or three (F) independent experiments *p < .05, **p < 0.01. Please also see Figures S1A–S1D.

vehicle only (Figure 2H). To validate this observation, we rescued the CSF1 depletion by intranasal instillation of bio-active recombinant CSF1 protein with DRA. In a dose-dependent manner (starting at 10 ng/mouse), intranasal instillation of recombinant CSF1 to the tamoxifen-injected *Scgb1a1-cre*ERT;*Csf1*$^{fl/fl}$ mice restored eosinophil recruitment into the lung and airways, the concentration of IL-4 and IL-13 in BAL fluids, as well as total and DRA-reactive serum IgE (Figures 2I, 2J, and S1G).

Inhibition of CSF1R Blocks IgE Production and Allergic Lung Inflammation in the DRA Asthma Model

The CSF1R is comprised of extracellular, transmembrane, and intracellular tyrosine kinase domains (Stanley and Chitu, 2014). Upon binding with ligand, the receptor undergoes phosphorylation at tyrosine residues in the intracellular domain. We determined that a selective CSF1R inhibitor, GW2580, had a strong pharmacologic binding affinity with K_D value of 1.77 ± 1.08 nM (Figure 3A). GW2580 completely blocked phosphorylation of CSF1R, whereas PLX647, another purported CSF1R inhibitor, showed only partial inhibition at Y546 (Figure 3A insert). Administration of GW2580 markedly suppressed eosinophil recruitment into the airways in a dose-dependent manner, starting at the lowest concentration (1 mg/kg) (Figure 3B), and significantly blocked asthmatic lung pathology and prevented the rise in total and DRA-reactive serum IgE and BAL IL-4 and IL-13 (Figures 3C–3E).

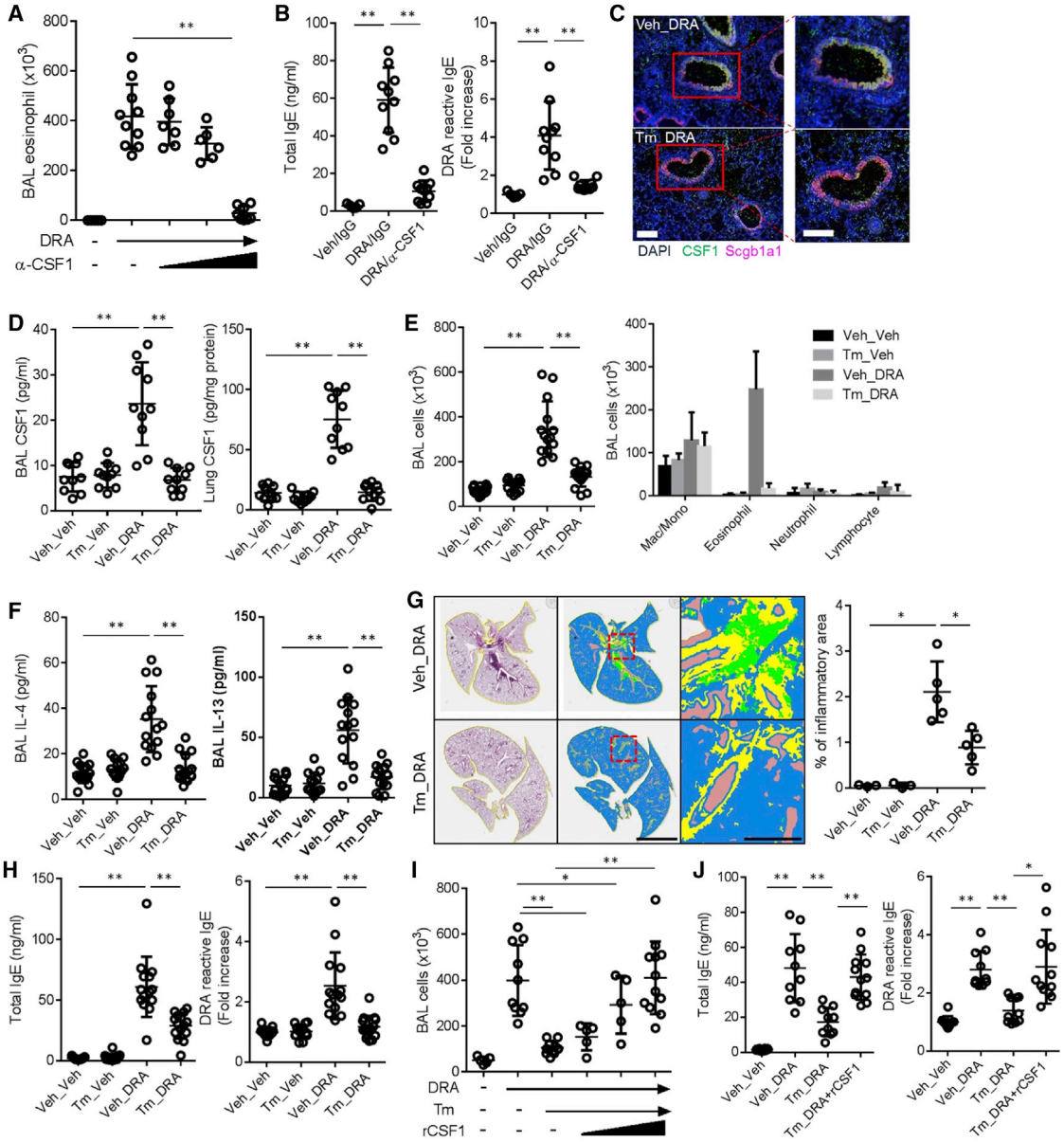

Figure 2. Deletion of CSF1 in Airway Epithelial Cells Blocks Allergen Sensitization and Subsequent Allergic Lung Inflammation

(A and B) Anti-CSF1 neutralizing antibody (α-CSF1, 1, 10, 100 ng/mouse, i.n.) was administered with DRA allergen during the challenge period (n = 6–10). The number of eosinophil in BAL and the total and DRA-reactive serum IgE were measured at the end of the DRA protocol.

(C and D) Immunofluorescence (IF) staining of lung from the *Scgb1a1-cre*ERT;*Csf1*$^{fl/fl}$ mice subjected to the DRA model with tamoxifen (Tm) or vehicle (Veh). Expression of CSF1 (green) was colocalized with Scgb1a1 (magenta) as shown by yellow cells in the merged image (scale bar = 100 μm). CSF1 was measured in BAL fluids and lung lysates.

(E–H) *Scgb1a1-cre*ERT;*Csf1*$^{fl/fl}$ mice were injected with either Tm or vehicle for five consecutive days (day 0–day 4) and subject to the DRA model (n = 9–15). Total and differential cell counts and the concentrations of IL-4 and IL-13 were measured in the BAL fluids. The colors in quantification of lung pathology indicate the following: green, inflammatory cells; yellow, area of the airway; brown, void space. Scale bars are 5 mm in middle and 500 μm in right panels. Total and DRA-reactive serum IgE were measured by ELISA.

(I and J) Rescue experiment of Tm-injected *Scgb1a1-cre*ERT;*Csf1*$^{fl/fl}$ with recombinant CSF1 (rCSF1, 0.1, 1, and 10 ng/mouse, i.n.) which was co-administered with DRA during challenge period.

Data in (A) and (B) are pooled data from two independent experiments and data in (C)–(J) are representative four independent experiments. *p < .05, **p < .01. Please also see Figures S1E–S1G.

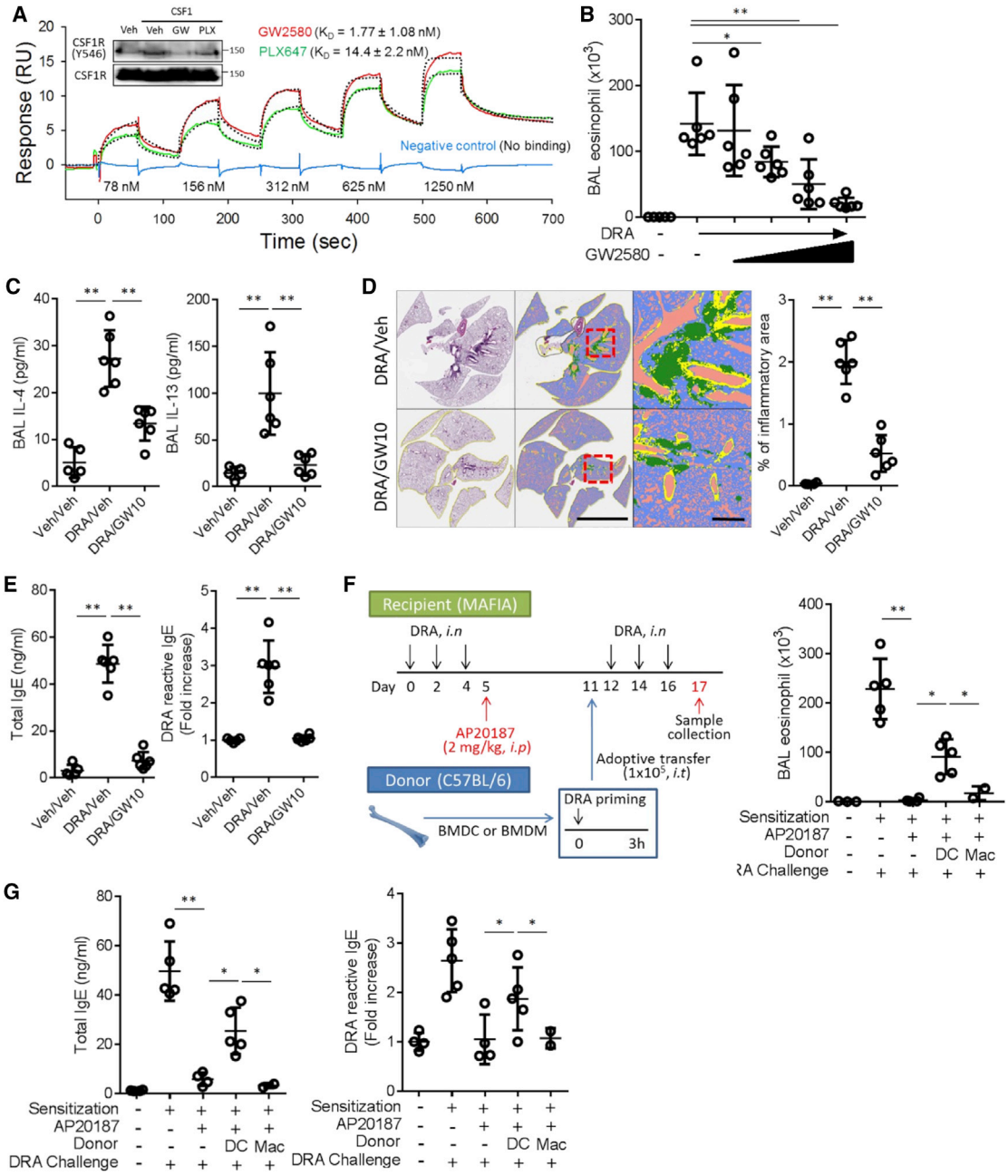

Figure 3. Inhibition of CSF1R Blocks IgE Production and Allergic Lung Inflammation in the DRA Asthma Model

(A) Surface plasmon resonance (SPR) binding analysis for CSF1R inhibitors (GW2580 and PLX647). Experimental sensorgrams (colored lines) were fitted by using a two-state reaction model, and the fitted curves are shown in the black dotted line. Phosphorylation of CSF1R at tyrosine 546 was measured at 20 min after CSF1 (10 ng/mL) stimulation with or without pre-treatment of CSF1 inhibitors (GW2580 and PLX647; each 1 μM) in RAW 264.7 cells.

(B) Increasing doses of GW2580 were injected during the DRA challenge period (0.01, 0.1, 1 to 10 mg/kg daily, i.p.). Eosinophil counts in BAL fluid were decreased in a dose-dependent manner.

(C–E) GW2580 (10 mg/kg, i.p.) was treated during challenge period of the DRA model and the degree of lung inflammation, the concentrations of BAL IL-4 and IL-13, total and DRA reactive serum IgE were measured. The colors in quantification of lung pathology indicates the following: green, inflammatory cells; yellow, area of the airway; purple, void space (n = 5–6). Scale bars are 5 mm in middle and 500 μm in right panels.

(F and G) Experimental scheme of adoptive transfer (i.t.) of DRA-pulsed DCs or macrophages to MAFIA mice (n = 2–5). $CSF1R^+$ cells in recipient mice were depleted by AP20187 injection after the DRA sensitization. Either the cultured DCs or macrophages were transferred intratracheally before the challenge phase. AP20187 abolished the eosinophilic recruitment and total and DRA reactive IgE production, which was partially restored by DC transfer but not by macrophage transfer.

Data in (A) are representative of three independent experiments and data in (B)–(G) are two independent experiments. *p < .05, **p < .01.

Our laboratory has shown that depletion of the CSF1R$^+$ cells using MAFIA mice, which carry *Csf1r* promoter-driven EGFP and suicidal *Fasl* genes, results in marked attenuation of allergic lung inflammation (Lee et al., 2015). Since DCs and macrophages are the two major CSF1R$^+$ cells, we examined which of these cells is crucial for CSF1-CSF1R pathway-mediated allergic inflammation. We performed adoptive transfer of bone marrow-derived DCs and macrophages in the DRA-induced asthma model as shown in Figure 3F. MAFIA mice were used for depletion of CSF1R$^+$ cells during the allergen challenge period. After the initial sensitization phase, injection of AP20187 depleted CSF1R$^+$ macrophages and DCs, resulting in a marked reduction of eosinophil recruitment into the airways (BAL fluid) and the total and DRA reactive serum IgE (Figures 3F and 3G). Intratracheal delivery of allergen-pulsed DCs to the CSF1R$^+$ cell-depleted MAFIA mice partially restored the rise in total and DRA-reactive serum IgE, as well as airway eosinophil recruitment after allergen challenge (Figures 3F and 3G), whereas adoptive transfer of DRA-pulsed macrophages (Mac) had no effect (Figures 3F and 3G), indicating that a functioning CSF1-CSF1R pathway of DCs is necessary for allergen-specific IgE production in allergic inflammation.

CSF1-CSF1R Pathway Regulates cDC2 Migration to Regional LNs in Allergic Lung Inflammation

Dendritic cells are potent antigen presenters found throughout the entire respiratory system. A small number of DCs also reside in the alveolar space in healthy and diseased human lungs (Kerrin et al., 2017; Yu et al., 2016). In a human subject who underwent SBP-AG, the numbers of total and CSF1R$^+$ cDCs in BAL fluid were increased at 48 hr after the allergen challenge (Figures 4A and 4B). By using the method of mass cytometry in conjunction with tSNE analysis, the total live cells from human BAL fluids were gated for the lineage-negative pool (CD3$^-$CD19$^-$CD56$^-$CD193$^-$Siglec8$^-$) and then gated for HLA-DR$^{+/++}$ and/or CD11c$^+$ (Figure S2). As shown in Figures 4A and 4B, both alveolar cDC1 (CD103$^+$) and cDC2 (CD1c$^+$) populations were found in pre-allergen-challenged samples (Pre), but the numbers of cDC2s, especially CSF1R$^+$cDC2s, were considerably more increased at 48 hr after the allergen challenge (Post), compared to the number of cDC1s (Figure 4B).

In the DRA asthma model, we analyzed the CSF1R positivity of cDC1s, cDC2s, and alveolar macrophages and found that the number of CSF1R$^+$ cDC2s was increased by the allergen challenge, whereas the CSF1R expression of cDC1s and alveolar macrophages was high at baseline and remained unchanged by allergen challenge (Figures 4C, S3A, and S3B). Next, to investigate whether AEC-derived CSF1 modulates the population and function of cDCs, we measured the total number of cDC subsets in BAL fluids and mLNs of *Scgb1a1-cre*ERT;*Csf1*$^{fl/fl}$. The DRA challenge increased the numbers of *both* CSF1R$^+$ cDC1s and cDC2s in the BAL fluids and mediastinal LNs in the DRA model (Figures 4D, 4E, S3C, and S3D). Compared to vehicle only, however, depletion of CSF1 by tamoxifen markedly reduced cDC2s in mediastinal LNs as well as conventional DCs (both cDC1s and cDC2s) in BAL fluids in *Scgb1a1-cre*ERT;*Csf1*$^{fl/fl}$ mice (Figures 4D and 4E), suggesting that epithelial-derived CSF1 is important in regulating the numbers of alveolar cDCs and the selective migration of cDC2s to the regional LNs. Notably, cDC2s are the principal DC subset shown to transport antigen to the LNs in HDM-induced allergic inflammation (Plantinga et al., 2013). To quantify the trafficking of allergen from the alveolar space to regional LNs, we utilized the fluorophore ZW800 conjugated to HDM (ZW-HDM) that allows *in vivo* tracking of allergen uptake in the DRA model (Choi et al., 2013). The mediastinal LNs were isolated after DRA challenge and the fluorescent dye (ZW) signal was measured in cDC2s by flow cytometry. There was a marked reduction in LN trafficking of the fluorescence-conjugated HDM in tamoxifen-injected *Scgb1a1-cre*ERT;*Csf1*$^{fl/fl}$ mice (Figure 4F). Furthermore, GW2580 blocked the migration of ZW-HDM$^+$ cDC2s to mediastinal LNs in a dose-dependent manner (Figure 4G). Collectively, these data demonstrate that AEC-derived CSF1 regulates LN migration of cDC2s.

IRF4 Expression in CSF1R$^+$ cDC2s Is Required for Allergic Inflammation

IRF4 regulates molecules central to cDC2 functions but does not alter the numbers and function of cDC1s (Bajaña et al., 2016). The expression of IRF4 in DCs is positively associated with increased antigen presentation capability (Roquilly et al., 2017). Th2 cell-promoting stimuli induce DC expression of IRF4 and the conditional depletion of IRF4 in DCs abolishes Th2 cell-type allergic lung inflammation (Williams et al., 2013). To investigate the expression of CSF1R-dependent IRF4, we instilled recombinant CSF1 (100 ng/mouse) into the lung. After 24 hr, the BAL cells were collected and analyzed for IRF4 expression. CSF1 enhanced the expression of IRF4 in alveolar CSF1R$^+$ DCs (Figure 5A). To examine the role of IRF4 in CSF1R$^+$ cells in allergic inflammation, we generated *Csf1r-cre*ERT;*Irf4* $^{fl/fl}$ mice. Tamoxifen injection ablated IRF4$^+$CSF1R$^+$ cells in the airway BAL fluid (Figure 5B, left). In the DRA model, tamoxifen-injected *Csf1r-cre*ERT;*Irf4* $^{fl/fl}$ mice showed significantly reduced CSF1R$^+$IRF4$^+$ cDC2s in the BAL fluid (Tm_DRA), compared to mice treated with DRA and vehicle (Veh_DRA) (Figure 5B, right). The asthmatic phenotype, including the serum IgE eosinophil recruitment into the BAL fluid and allergic lung inflammation, was markedly attenuated in the tamoxifen-treated group (Figures 5C–5E). The Tm cell injection also suppressed the LN migration of ZW-HDM$^+$ cDC2s to mLN in the DRA model (Figure 5F). To ascertain the role of cDC2s in this mouse, we conducted an adoptive transfer experiment of sorted cDC2s. First, CSF1R$^+$IRF4$^+$ cells were depleted by tamoxifen injection, and then we restored only the cDC2 population by adoptive transfer of flow cytometry-purified lung cDC2s (CD45$^+$CD11c$^+$CD172a$^+$F4/80$^-$CD64$^-$XCR1$^-$). The adoptive transfer of lung cDC2s significantly rescued serum concentrations of both total and allergen-specific IgE. In contrast, the donor lung cDC2s treated by either anti-CSF1R antibody or GW2580 (1 μM) before adoptive transfer were unable to rescue the production of IgE (Figures 5G and 5H). Collectively, these data support the concept that CSF1R on cDC2s plays a key role in this mouse asthma model.

CSF1-CSF1R Pathway Facilitates LN Migration of Alveolar DCs through Upregulation of CCR7 Expression

To investigate whether CSF1 has a direct effect on antigen presentation and IgE production per se, splenocytes were cultured and stimulated with DRA in the presence or absence of CSF1. The concentration of IgE in the culture media was increased by

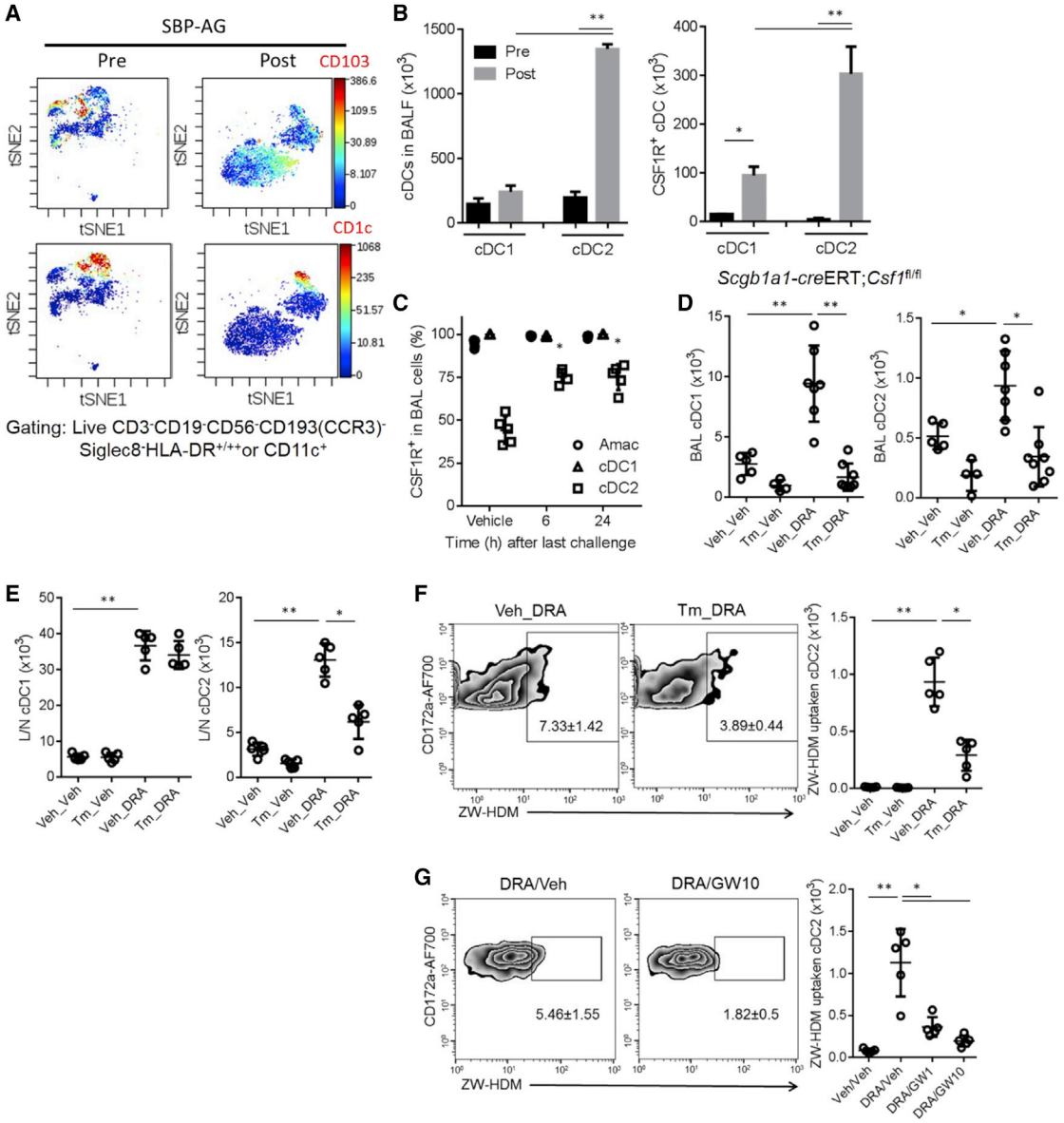

Figure 4. CSF1-CSF1R Pathway Promotes Alveolar cDC2 Migration to Regional LNs

(A and B) Mass cytometry of human BAL cells before (Pre) and at 48 hr (Post) after allergen challenge. From the cDC gated population, the numbers of cDC1s, cDC2s, and CSF1R$^+$ cells were calculated.

(C) The percentage of CSF1R$^+$ cells among alveolar macrophages (Amac), cDC1s, and cDC2s were measured with or without DRA challenges in the BAL fluids at 6 and 24 hr after last challenge.

(D and E) Number of CSF1R$^+$ cDC1s and cDC2s in BAL fluid and mediastinal LNs with DRA challenge or vehicle in *Scgb1a1-cre*ERT;*Csf1*$^{fl/fl}$ with or without Tm injection.

(F and G) Fluorophore ZW800-conjugated HDM (ZW-HDM) was measured in the mediastinal LNs in the DRA asthma model. After gating to the CD172a$^+$ cDC2 population, the ZW-HDM$^+$ cells were counted in *Scgb1a1-cre*ERT;*Csf1*$^{fl/fl}$ mice with or without Tm injection in the presence or absence of GW2580 (10 mg/kg, i.p.).

Data in (C)–(G) are at least two independent experiments. *p < .05, **p < .01. Please also see Figures S2 and S3.

DRA treatment on day 3 and further increased on day 7, but the addition of CSF1 had no effect on IgE production (Figure S4A). These data suggest that CSF1 influences these events prior to LN arrival of antigen.

In order to examine whether the CSF1-CSF1R pathway regulates cDC migration to LNs *in vivo*, we conducted an intratracheal (i.t.) adoptive transfer of cultured DCs. EGFP$^+$ donor DCs were harvested from MAFIA mice that express *Csf1r* promoter-driven EGFP, cultured with IL-4 (10 ng/mL) for 6 hr, and transferred to recipients on day 11 of the DRA model. Then, DRA with or without anti-CSF1 antibody (100 ng/mouse) was used to challenge the DRA-sensitized recipient mice on day 12. The

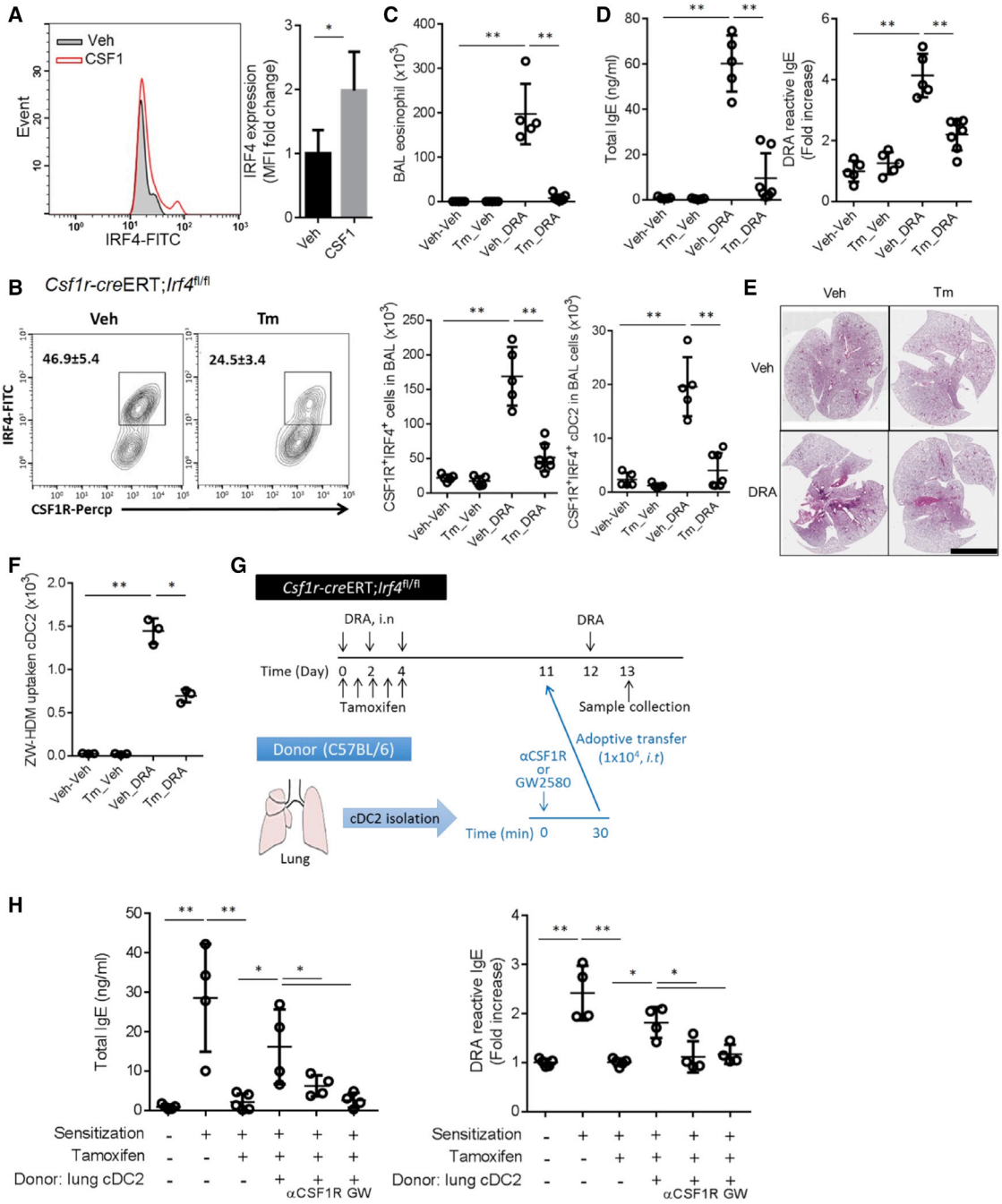

Figure 5. IRF4 Expression in CSF1R⁺ cDC2s Is Required for Allergic Inflammation

(A) Recombinant CSF1 (10 ng/mouse, i.n.) was administered and BAL cells were collected after 24 hr. CD11c⁺ F4/80⁻CSF1R⁺ DCs were gated and the intensity of IRF4 was measured.

(B) *Csf1r-cre*ERT;*Irf4*$^{fl/fl}$ mice were treated with either Tm or vehicle for five consecutive days (day 0–day 4) of the DRA model. The number of CSF1R⁺IRF4⁺ cells and CSF1R⁺IRF4⁺ cDC2s in the BAL fluids of *Csf1r-cre*ERT;*Irf4*$^{fl/fl}$ mice in the DRA asthma model with and without tamoxifen (Tm).

(C–F) The number of BAL eosinophils, serum total, and DRA-reactive IgE, the degree of lung inflammation and migration of ZW-HDM⁺ cDC2s to mediastinal LNs were measured. Scale bar is 5 mm.

(G) Experimental scheme of adoptive transfer (i.t.) of lung cDC2s to the recipient mice which were DRA-sensitized, Tm-injected *Csf1r-cre*ERT;*Irf4*$^{fl/fl}$ mice (n = 4–5).

(H) Total and DRA-reactive serum IgE were measured by ELISA.

Data represent at least two (A–F) independent experiments. *p < .05, **p < .01.

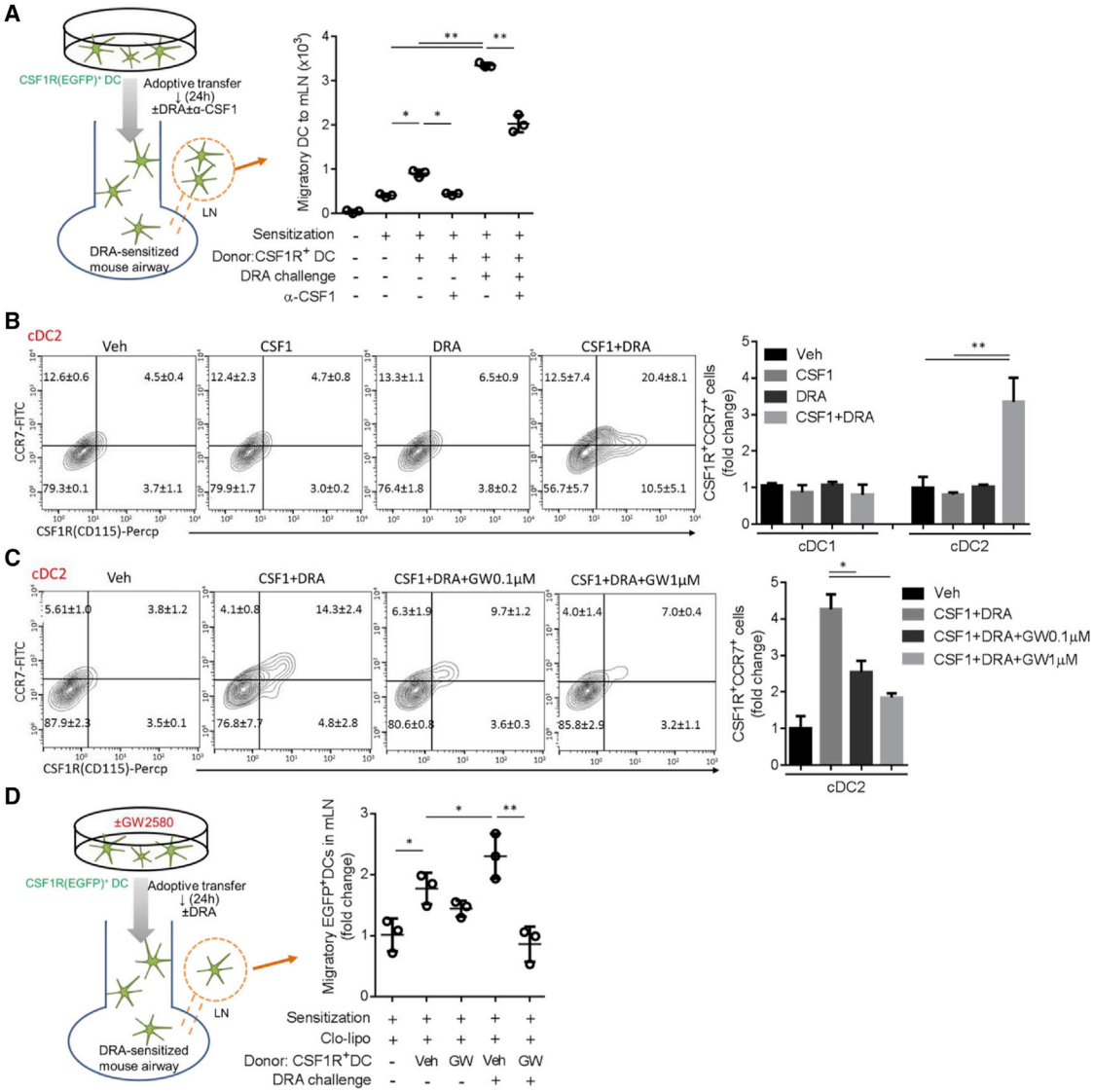

Figure 6. CSF1-CSF1R Pathway Facilitates LN Migration of Alveolar DCs through Upregulation of CCR7 Expression

(A) Experimental scheme of adoptive transfer of EGFP$^+$ DCs. After intranasal sensitization, EGFP$^+$ BMDCs were adoptively transferred to the DRA-sensitized mice on day 11 with or without concomitant intranasal anti-CSF1 antibody (100 ng/mouse). The number of migratory DCs to mLN was measured by flow cytometry.

(B and C) Single-cell suspension from lung was cultured and stimulated with CSF1 and/or DRA for 24 hr. The expressions of CSF1R and CCR7 on cDC2s were measured by flow cytometry. However, GW2580 treatment effectively blocked the increase of CSF1R$^+$CCR7$^+$ cells in a dose-responsive manner in the combined treatment with DRA and CSF1.

(D) After intranasal sensitization, myeloid cells in recipient lung were depleted by clodronate liposome. The intratracheal adoptive transfer of EGFP$^+$ DCs was performed with or without GW2580 treatment for 1 hr. The number of migratory EGFP$^+$ DCs was measured at mLN by flow cytometry.

Data represent at least two independent experiments. *p < .05, **p < .01. Please also see Figures S4–S6.

number of EGFP$^+$ donor DCs were measured in mLNs at the end of the protocol (Figure S4B). The DRA challenge boosted DC migration to the LNs, which was significantly attenuated by the simultaneous treatment with anti-CSF1 antibody (Figures 6A, S4C, and S4D). Accordingly, total and DRA-reactive serum IgE were significantly reduced in the anti-CSF1 antibody-treated group (Figure S4E).

CCR7 mediates DC migration to LNs and the depletion of CCR7 can abolish allergic lung inflammation (Ohl et al., 2004; Worbs et al., 2017). To examine whether CSF1 regulated CCR7 expression on DCs, a single-cell suspension of lung was made and cultured in the presence of recombinant CSF1 with or without DRA stimuli for 24 hr. These cells were immunostained and gated for separation into cDC1 and cDC2 populations and the expression of CCR7 and CSF1R was analyzed (Figures S5A and S5B). Of interest, the CSF1R$^+$CCR7$^+$ cDC2 population was low (4.5%) at baseline but was increased by the combined treatment with CSF1 and DRA (20.4%), whereas individually, CSF1 and DRA treatment had no effect (Figure 6B). In contrast, CSF1R$^+$CCR7$^+$ cDC1s were high at baseline (73.1%) and was

unchanged by the stimuli (Figure S5C). Notably, GW2580 treatment blocked the rise of $CCR7^+$ and $CSF1R^+$ cells in a dose-responsive manner in the DRA- and CSF1-treated group (Figure 6C).

Since the CSF1R inhibitor blocked CCR7 expression on cDC2s, we determined the effect of GW2580 on the LN migration of DCs. As depicted in Figures S6A and S6B, $EGFP^+$ DCs were harvested from MAFIA mice and cultured in the presence of IL-4 (10 ng/mL) for 6 hr and GW2580 (0.5 μM) added for the last hour of culture. Before receiving donor cells, all recipient mice were sensitized with DRA allergen and then treated with clodronated liposomes on day 10 to deplete intrinsic myeloid lineage cells. DRA challenge increased the LN migration of the $EGFP^+$ donor DCs, compared to the unchallenged mice. However, inhibition of CSF1R signaling by GW2580 markedly reduced the number of LN migrated $EGFP^+$ donor DCs as well as the DRA-reactive serum IgE and the number of airway eosinophils in BAL (Figures 6D and S6C–S6E). These data indicate that the CSF1-CSF1R pathway regulates CCR7 expression that facilitates LN migration of alveolar cDC2s.

DISCUSSION

The SBP-AG model is a strong research tool for examining the Th2 cell-mediated immune response in human asthma. Unlike cross-sectional population-based asthma studies, which are limited by the heterogeneity of asthma phenotypes and genetic variability, SBP-AG offers a chronological view of what happens to lung micro-environments after allergen exposure in a single atopic individual with asthma (Park et al., 2013). The SBP-AG protocol allows measurement of cellular, biochemical, and immunological alterations in the lung micro-environment within a 48 hr window after allergen challenge in human asthmatics (Lee et al., 2015). By using this protocol, we have shown that monocyte-derived macrophages are actively recruited to alveolar space in a CCL2-CCR2-dependent manner.

CSF1 is a pleiotropic cytokine regulating diverse cell functions. Although its signal converges on the CSF1 receptor expressed mainly on myeloid lineage cells, CSF1 is produced by various types of structural cells both *in vivo* and under *in vitro* conditions (Fixe and Praloran, 1998), suggesting that it is a link between non-myeloid and innate immune myeloid effector cells. Recent studies indicate that structural cells secrete CSF1 in response to tissue damage, which plays a role as an early danger signal that maintains regional homeostasis. For example, CSF1 is markedly and selectively induced in injured sensory neurons and is transported to the spinal cord where it induces microglial activation and mechanical hypersensitivity of neurons. In acute kidney injury, proximal tubule-producing CSF1 is essential for recovery of injured kidney (Guan et al., 2016; Wang et al., 2015). Upon allergen challenge, we found that CSF1 was consistently increased in the BAL fluids from SBP-AG subjects 48 hr after challenge. On average, the concentration of CSF1 in post-allergen-challenged BAL fluid was markedly increased, an average of 18-fold, ranging from increase of 3- to 47-fold. These data indicate that the allergic lung microenvironmental milieu is enriched with CSF1 by allergen challenge.

Our human SBP-AG data as well as the data from the murine DRA model of allergic asthma showed that there is recruitment of alveolar DCs in response to allergen challenge. Although CSF1 is known to have an *in vitro* chemotactic activity for macrophages through activation of the PI3K and Akt pathway, we observed that intratracheal instillation of CSF1 (up to 100 ng/mouse) had no effect on DC recruitment to the airspaces in a stimulus-free naive mouse and an *in vitro* chemotactic assay of CSF1 for DCs failed to show directional migration in the experimental setting (data not shown). CSF1 has been shown to indirectly recruit $Ly6C^{hi}$ monocytes through the induction a macrophage chemokine, CCL2, in inflammatory and non-inflammatory conditions (Baran et al., 2007). The extravasation of $CSF1R^+$ pre-DCs was blocked by pertussis toxin which inhibits G-protein coupled chemokine receptors, but not the CSF1R (Tagliani et al., 2011). These findings imply that CSF1 may induce other DC-attracting chemokines involved in $CSF1R^+$ cell recruitment. It is also possible that reduced DC recruitment in CSF1-deficient mice could simply be secondary to decreased IgE production. Atopic asthma is basically an IgE-mediated allergic inflammation and decreased IgE production is expected to lead to decreased mast cell and basophil activation, thus limiting the development of airway inflammation, the recruitment of inflammatory cells such as eosinophils, and decreased production of chemokines and cytokines (Holgate et al., 2005).

Airway DCs in conducting airway are known to be located beneath airway epithelial cells and to extend their processes into the airway lumen across the epithelium (Hammad et al., 2009). However, a recent study shows that only 3% of airway DCs generated processes in this way in allergen-challenge mice and none of them had a dendrite process past the outermost epithelium into the lumen, which raises the question of their capability to detect antigen (Thornton et al., 2012). In this report, we delivered cultured DCs directly into the airways and traced their migration into the regional LN. Trans-epithelial migration of DCs to the luminal surface of the alveolar space has been reported, and alveolar DCs demonstrated extended dendrites moving along the luminal surface of alveolar epithelial cells to sample antigen (Thornton et al., 2012). In SBP-AG subjects, alveolar DCs were increased in number and differentially expressed protein markers in response to allergen challenge. It would be intriguing to study differences in phenotype between pre- and post-allergen-challenged cDCs.

DC immigration to a draining LN requires the chemokine receptor CCR7 (Worbs et al., 2017). IRF4 not only regulates antigen presentation, but also plays a crucial role for the CCR7-mediated migration of DCs, especially the cDC2 population. IRF4-deficient $CD11b^+$ cDC2s do not express CCR7 and fail to migrate to a regional LN, and mice deficient in IRF4 in $CD11c^+$ cells showed significant attenuation of allergic lung inflammation (Bajaña et al., 2012; Williams et al., 2013). Our data show that CSF1-induced IRF4 expression in the DC population and the depletion of IRF4 in $CSF1R^+$ cells blocks the migration of allergen-induced cDC2s. CSF1 is a coactivator for the mTORC2 signaling pathway and its downstream activation, and IRF4 expression is dependent on CSF1-mTORC2 activation (Huang et al., 2016). Considering that mTORC2 plays a vital role in cell motility and the cytoskeleton, our data suggest that the CSF1-mTORC2-IRF4 pathway is important for CCR7-mediated DC migration. In addition to upregulation of CCR7, DC migration also requires priming signals from cytokines coming from

activation of the inflammasome (Ichinohe et al., 2011). In influenza virus infection, IL-1 and IL-18 induced by commensal bacteria plays a role as the priming signal, and the eradication of commensal bacteria by antibiotic treatment impairs DC migration to the draining LN. IL-1R controls CCR7 expression and migration of lung DCs (Pang et al., 2013). We have determined that AECs recognize aeroallergen and provide CSF1 to prime cDC2s by inducing CCR7 expression in the process of DC transport of aeroallergen and subsequent antigen presentation.

IgE production in IgE-mediated allergic inflammation is not a single step process, but requires initial sensitization and boosting by repeated allergen challenge. Serum IgE decreases rapidly upon cessation of exposure to allergen (Brightbill et al., 2010; Talay et al., 2012). In order to maintain IgE amount, it is necessary to have allergen presentation that is mediated by cDC2s. By blocking the CSF1-CSF1R pathway, we were able to prevent the delivery of inhaled aeroallergen to the LNs for antigen presentation, resulting in a failure to boost IgE in previously sensitized mice. Thus, interdiction in the CSF1-CSF1R pathway has therapeutic implications in the setting where avoidance of aeroallergen is not possible. Preventing IgE elevation could have a therapeutic advantage over the current approach of immune absorbance of IgE in patients with refractory allergic asthma.

In summary, allergen challenge drives innate immune cells into the airway lumen. Our data suggest that airway epithelial cells have a key role in regulating DC function in the airspaces. DCs bridge innate and adaptive immune responses by mobilization of allergens and their presentation to adaptive immune cells. Epithelial-secreted CSF1 regulates DCs for trafficking aeroallergen and subsequent development of adaptive immune responses. Targeting the CSF1 pathway, which harnesses both the innate and adaptive arms of the immune system, could produce better outcomes for patients with uncontrolled allergic asthma.

STAR★METHODS

Detailed methods are provided in the online version of this paper and include the following:

SUPPLEMENTAL INFORMATION

Supplemental Information includes six figures and can be found with this article online at https://doi.org/10.1016/j.immuni.2018.06.009.

ACKNOWLEDGMENTS

We thank all of the generous asthmatic subjects who volunteered for the SBP-AG protocol, and the entire staff of the Clinical Research Core, Research Resource Center (Histology Core and Flow Cytometry Core) at the University of Illinois Center for Clinical and Translational Sciences (CCTS). We also thank Eleanor Rivera, R.N., and Drs. H. Ari Jaffe and Sharmilee Nyenhuis for assistance with the SBP-AG protocol. This work was supported by NIH grant R01HL126852 and Respiratory Health Association Grant (RHA2016-01-Lung Cancer) (to G.Y.P.) and in part by NIH grants R01 HL137224 (to J.W.C.), R01 AG045040 (to S.L.A.-W.), and P01 HL088594 (to N.N.J.). Performance of the SGP-AG protocol was supported in part by a pilot grant from the UIC CCTS (to S.J.A.).

AUTHOR CONTRIBUTIONS

H.-G.M. performed the mouse and cellular experiments, analyzed data, and drafted the manuscript. S.K. and S.-S.H. assisted the mouse and cellular experiments. J.J.J. measured the cytokines of human BAL fluids and generated the transgenic mice. N.N.J. provided BAL fluids and plasma from the Wisconsin cohort. S.L.A.-W. provided *Csf1*$^{fl/fl}$ mice. S.C. assisted in the generation of *Csf1r-cre*ERT;*Irf4*$^{fl/fl}$ mice. H.L. performed the SPR for CSF1R inhibitors and performed the ligand-docking simulations. H.S.C. provided fluorescent dye ZW800-conjugated HDM (ZW-HDM). S.J.A., V.N., and J.W.C. supported the SBP-AG protocol and assisted with data analyses. G.Y.P. conceptualized and supervised the study. H.-G.M., S.K., S.J.A., and G.Y.P. wrote the manuscript, with editing and feedback from all of the authors.

DECLARATION OF INTERESTS

H.-G.M. and G.Y.P. have filed a patent application related to this work.

Received: March 1, 2018
Revised: April 25, 2018
Accepted: June 21, 2018
Published: July 24, 2018

REFERENCES

Bajaña, S., Roach, K., Turner, S., Paul, J., and Kovats, S. (2012). IRF4 promotes cutaneous dendritic cell migration to lymph nodes during homeostasis and inflammation. J. Immunol. *189*, 3368–3377.

Bajaña, S., Turner, S., Paul, J., Ainsua-Enrich, E., and Kovats, S. (2016). IRF4 and IRF8 act in CD11c+ cells to regulate terminal differentiation of lung tissue dendritic cells. J. Immunol. *196*, 1666–1677.

Baran, C.P., Opalek, J.M., McMaken, S., Newland, C.A., O'Brien, J.M., Jr., Hunter, M.G., Bringardner, B.D., Monick, M.M., Brigstock, D.R., Stromberg, P.C., et al. (2007). Important roles for macrophage colony-stimulating factor, CC chemokine ligand 2, and mononuclear phagocytes in the pathogenesis of pulmonary fibrosis. Am. J. Respir. Crit. Care Med. *176*, 78–89.

Becher, B., Schlitzer, A., Chen, J., Mair, F., Sumatoh, H.R., Teng, K.W., Low, D., Ruedl, C., Riccardi-Castagnoli, P., Poidinger, M., et al. (2014). High-dimensional analysis of the murine myeloid cell system. Nat. Immunol. *15*, 1181–1189.

Brightbill, H.D., Jeet, S., Lin, Z., Yan, D., Zhou, M., Tan, M., Nguyen, A., Yeh, S., Delarosa, D., Leong, S.R., et al. (2010). Antibodies specific for a segment of

human membrane IgE deplete IgE-producing B cells in humanized mice. J. Clin. Invest. *120*, 2218–2229.

Choi, H.S., Gibbs, S.L., Lee, J.H., Kim, S.H., Ashitate, Y., Liu, F., Hyun, H., Park, G., Xie, Y., Bae, S., et al. (2013). Targeted zwitterionic near-infrared fluorophores for improved optical imaging. Nat. Biotechnol. *31*, 148–153.

Desch, A.N., Gibbings, S.L., Goyal, R., Kolde, R., Bednarek, J., Bruno, T., Slansky, J.E., Jacobelli, J., Mason, R., Ito, Y., et al. (2016). Flow cytometric analysis of mononuclear phagocytes in nondiseased human lung and lung-draining lymph nodes. Am. J. Respir. Crit. Care Med. *193*, 614–626.

Fixe, P., and Praloran, V. (1998). M-CSF: haematopoietic growth factor or inflammatory cytokine? Cytokine *10*, 32–37.

Fu, P., Mohan, V., Mansoor, S., Tiruppathi, C., Sadikot, R.T., and Natarajan, V. (2013). Role of nicotinamide adenine dinucleotide phosphate-reduced oxidase proteins in *Pseudomonas aeruginosa*-induced lung inflammation and permeability. Am. J. Respir. Cell Mol. Biol. *48*, 477–488.

Guan, Z., Kuhn, J.A., Wang, X., Colquitt, B., Solorzano, C., Vaman, S., Guan, A.K., Evans-Reinsch, Z., Braz, J., Devor, M., et al. (2016). Injured sensory neuron-derived CSF1 induces microglial proliferation and DAP12-dependent pain. Nat. Neurosci. *19*, 94–101.

Guilliams, M., and Scott, C.L. (2017). Does niche competition determine the origin of tissue-resident macrophages? Nat. Rev. Immunol. *17*, 451–460.

Hammad, H., Chieppa, M., Perros, F., Willart, M.A., Germain, R.N., and Lambrecht, B.N. (2009). House dust mite allergen induces asthma via Toll-like receptor 4 triggering of airway structural cells. Nat. Med. *15*, 410–416.

Hammad, H., Plantinga, M., Deswarte, K., Pouliot, P., Willart, M.A.M., Kool, M., Muskens, F., and Lambrecht, B.N. (2010). Inflammatory dendritic cells–not basophils–are necessary and sufficient for induction of Th2 immunity to inhaled house dust mite allergen. J. Exp. Med. *207*, 2097–2111.

Harris, S.E., MacDougall, M., Horn, D., Woodruff, K., Zimmer, S.N., Rebel, V.I., Fajardo, R., Feng, J.Q., Gluhak-Heinrich, J., Harris, M.A., and Abboud Werner, S. (2012). Meox2Cre-mediated disruption of CSF-1 leads to osteopetrosis and osteocyte defects. Bone *50*, 42–53.

Holgate, S., Casale, T., Wenzel, S., Bousquet, J., Deniz, Y., and Reisner, C. (2005). The anti-inflammatory effects of omalizumab confirm the central role of IgE in allergic inflammation. J. Allergy Clin. Immunol. *115*, 459–465.

Huang, S.C., Smith, A.M., Everts, B., Colonna, M., Pearce, E.L., Schilling, J.D., and Pearce, E.J. (2016). Metabolic reprogramming mediated by the mTORC2-IRF4 signaling axis is essential for macrophage alternative activation. Immunity *45*, 817–830.

Ichinohe, T., Pang, I.K., Kumamoto, Y., Peaper, D.R., Ho, J.H., Murray, T.S., and Iwasaki, A. (2011). Microbiota regulates immune defense against respiratory tract influenza A virus infection. Proc. Natl. Acad. Sci. USA *108*, 5354–5359.

Joffre, O., Nolte, M.A., Spörri, R., and Reis e Sousa, C. (2009). Inflammatory signals in dendritic cell activation and the induction of adaptive immunity. Immunol. Rev. *227*, 234–247.

Karpurapu, M., Wang, X., Deng, J., Park, H., Xiao, L., Sadikot, R.T., Frey, R.S., Maus, U.A., Park, G.Y., Scott, E.W., and Christman, J.W. (2011). Functional PU.1 in macrophages has a pivotal role in NF-κB activation and neutrophilic lung inflammation during endotoxemia. Blood *118*, 5255–5266.

Kerrin, A., Fitch, P., Errington, C., Kerr, D., Waxman, L., Riding, K., McCormack, J., Mehendele, F., McSorley, H., MacKenzie, K., et al. (2017). Differential lower airway dendritic cell patterns may reveal distinct endotypes of RSV bronchiolitis. Thorax *72*, 620–627.

Lambrecht, B.N., and Hammad, H. (2012). The airway epithelium in asthma. Nat. Med. *18*, 684–692.

Lee, Y.G., Jeong, J.J., Nyenhuis, S., Berdyshev, E., Chung, S., Ranjan, R., Karpurapu, M., Deng, J., Qian, F., Kelly, E.A., et al. (2015). Recruited alveolar macrophages, in response to airway epithelial-derived monocyte chemoattractant protein 1/CCl2, regulate airway inflammation and remodeling in allergic asthma. Am. J. Respir. Cell Mol. Biol. *52*, 772–784.

MacDonald, K.P., Rowe, V., Bofinger, H.M., Thomas, R., Sasmono, T., Hume, D.A., and Hill, G.R. (2005). The colony-stimulating factor 1 receptor is expressed on dendritic cells during differentiation and regulates their expansion. J. Immunol. *175*, 1399–1405.

Madisen, L., Zwingman, T.A., Sunkin, S.M., Oh, S.W., Zariwala, H.A., Gu, H., Ng, L.L., Palmiter, R.D., Hawrylycz, M.J., Jones, A.R., et al. (2010). A robust and high-throughput Cre reporting and characterization system for the whole mouse brain. Nat. Neurosci. *13*, 133–140.

Moon, H.G., Tae, Y.M., Kim, Y.S., Gyu Jeon, S., Oh, S.Y., Song Gho, Y., Zhu, Z., and Kim, Y.K. (2010). Conversion of Th17-type into Th2-type inflammation by acetyl salicylic acid via the adenosine and uric acid pathway in the lung. Allergy *65*, 1093–1103.

Moon, H.G., Cao, Y., Yang, J., Lee, J.H., Choi, H.S., and Jin, Y. (2015). Lung epithelial cell-derived extracellular vesicles activate macrophage-mediated inflammatory responses via ROCK1 pathway. Cell Death Dis. *6*, e2016.

Ohl, L., Mohaupt, M., Czeloth, N., Hintzen, G., Kiafard, Z., Zwirner, J., Blankenstein, T., Henning, G., and Förster, R. (2004). CCR7 governs skin dendritic cell migration under inflammatory and steady-state conditions. Immunity *21*, 279–288.

Pang, I.K., Ichinohe, T., and Iwasaki, A. (2013). IL-1R signaling in dendritic cells replaces pattern-recognition receptors in promoting $CD8^+$ T cell responses to influenza A virus. Nat. Immunol. *14*, 246–253.

Park, G.Y., Lee, Y.G., Berdyshev, E., Nyenhuis, S., Du, J., Fu, P., Gorshkova, I.A., Li, Y., Chung, S., Karpurapu, M., et al. (2013). Autotaxin production of lysophosphatidic acid mediates allergic asthmatic inflammation. Am. J. Respir. Crit. Care Med. *188*, 928–940.

Patel, V.I., Booth, J.L., Duggan, E.S., Cate, S., White, V.L., Hutchings, D., Kovats, S., Burian, D.M., Dozmorov, M., and Metcalf, J.P. (2017). Transcriptional classification and functional characterization of human airway macrophage and dendritic cell subsets. J. Immunol. *198*, 1183–1201.

Plantinga, M., Guilliams, M., Vanheerswynghels, M., Deswarte, K., Branco-Madeira, F., Toussaint, W., Vanhoutte, L., Neyt, K., Killeen, N., Malissen, B., et al. (2013). Conventional and monocyte-derived CD11b(+) dendritic cells initiate and maintain T helper 2 cell-mediated immunity to house dust mite allergen. Immunity *38*, 322–335.

Rivera, A., Siracusa, M.C., Yap, G.S., and Gause, W.C. (2016). Innate cell communication kick-starts pathogen-specific immunity. Nat. Immunol. *17*, 356–363.

Roquilly, A., McWilliam, H.E.G., Jacqueline, C., Tian, Z., Cinotti, R., Rimbert, M., Wakim, L., Caminschi, I., Lahoud, M.H., Belz, G.T., et al. (2017). Local modulation of antigen-presenting cell development after resolution of pneumonia induces long-term susceptibility to secondary infections. Immunity *47*, 135–147.e5.

Shin, E.K., Lee, S.H., Cho, S.H., Jung, S., Yoon, S.H., Park, S.W., Park, J.S., Uh, S.T., Kim, Y.K., Kim, Y.H., et al. (2010). Association between colony-stimulating factor 1 receptor gene polymorphisms and asthma risk. Hum. Genet. *128*, 293–302.

Stanley, E.R., and Chitu, V. (2014). CSF-1 receptor signaling in myeloid cells. Cold Spring Harb. Perspect. Biol. *6*, 6.

Tagliani, E., Shi, C., Nancy, P., Tay, C.-S., Pamer, E.G., and Erlebacher, A. (2011). Coordinate regulation of tissue macrophage and dendritic cell population dynamics by CSF-1. J. Exp. Med. *208*, 1901–1916.

Talay, O., Yan, D., Brightbill, H.D., Straney, E.E., Zhou, M., Ladi, E., Lee, W.P., Egen, J.G., Austin, C.D., Xu, M., and Wu, L.C. (2012). IgE^+ memory B cells and plasma cells generated through a germinal-center pathway. Nat. Immunol. *13*, 396–404.

Thornton, E.E., Looney, M.R., Bose, O., Sen, D., Sheppard, D., Locksley, R., Huang, X., and Krummel, M.F. (2012). Spatiotemporally separated antigen uptake by alveolar dendritic cells and airway presentation to T cells in the lung. J. Exp. Med. *209*, 1183–1199.

Wang, Y., Chang, J., Yao, B., Niu, A., Kelly, E., Breeggemann, M.C., Abboud Werner, S.L., Harris, R.C., and Zhang, M.Z. (2015). Proximal tubule-derived colony stimulating factor-1 mediates polarization of renal macrophages and dendritic cells, and recovery in acute kidney injury. Kidney Int. *88*, 1274–1282.

Whitsett, J.A., and Alenghat, T. (2015). Respiratory epithelial cells orchestrate pulmonary innate immunity. Nat. Immunol. *16*, 27–35.

Willart, M.A.M., Deswarte, K., Pouliot, P., Braun, H., Beyaert, R., Lambrecht, B.N., and Hammad, H. (2012). Interleukin-1α controls allergic sensitization to inhaled house dust mite via the epithelial release of GM-CSF and IL-33. J. Exp. Med. *209*, 1505–1517.

Williams, J.W., Tjota, M.Y., Clay, B.S., Vander Lugt, B., Bandukwala, H.S., Hrusch, C.L., Decker, D.C., Blaine, K.M., Fixsen, B.R., Singh, H., et al. (2013). Transcription factor IRF4 drives dendritic cells to promote Th2 differentiation. Nat. Commun. *4*, 2990.

Worbs, T., Hammerschmidt, S.I., and Förster, R. (2017). Dendritic cell migration in health and disease. Nat. Rev. Immunol. *17*, 30–48.

Yu, Y.R., Hotten, D.F., Malakhau, Y., Volker, E., Ghio, A.J., Noble, P.W., Kraft, M., Hollingsworth, J.W., Gunn, M.D., and Tighe, R.M. (2016). Flow cytometric analysis of myeloid cells in human blood, bronchoalveolar lavage, and lung tissues. Am. J. Respir. Cell Mol. Biol. *54*, 13–24.

STAR★METHODS

KEY RESOURCES TABLE

REAGENT or RESOURCE	SOURCE	IDENTIFIER
Antibodies		
Anti-human CD19	Fluidigm	HIB19, cat#3142001B; RRID: AB_2651155
Anti-human CD11b	Fluidigm	ICRF44, cat#3144001B; RRID: AB_2714152
Anti-human CD11c	Fluidigm	Bu15, cat#3159001B; RRID: AB_2687635
Anti-human CD7	Fluidigm	CD7-6B7, cat#3147006B
Anti-human CD66a	Fluidigm	CD66a-B1.1, cat#3149008B
Anti-human CD68	Fluidigm	Y1/82A, cat#6171011B; RRID: AB_2687637
Anti-human CD163	Fluidigm	GHI/64, cat#3154007B; RRID: AB_2661797
Anti-human CD45	Fluidigm	HI30, cat#3156010B; RRID: AB_2714154
Anti-human CD14	Fluidigm	M5E2, cat#3160001B; RRID: AB_2687634
Anti-human CD16	Fluidigm	3G8, cat#3165001B; RRID: AB_2661791
Anti-human CD38	Fluidigm	HIT2, cat#3167001B; RRID: AB_2687640
Anti-human CD206	Fluidigm	15-2, cat#3168008B; RRID: AB_2661805
Anti-human CD33	Fluidigm	WM53, cat#3169010B; RRID: AB_2661799
Anti-human CD3	Fluidigm	UCHT1, cat#3170001B; RRID: AB_2687853
Anti-human HLA-DR	Fluidigm	L243, cat#3174001B; RRID: AB_2665397
Anti-human CD193	Fluidigm	5E8, cat#3175025B
Anti-human Siglec-8	Fluidigm	7C9, cat#316407B
Anti-human CD86	Fluidigm	IT2.2, cat#3150020B; RRID: AB_2661798
Anti-human CD123	Fluidigm	6H6, cat#3143014; RRID: AB_2661794
Anti-human CX3CR1	Fluidigm	2A9-1, cat#3172017B
Anti-human CD64	Fluidigm	10.1, cat#3154007B
Anti-human CD31	Fluidigm	WM59, cat#3145004B
Anti-human CD103	Fluidigm	Ber-ACT8, cat#3151011B
Anti-human CD26	Fluidigm	BA5b, cat#3161015B
Anti-human CD127	Fluidigm	A019D5, cat#3176004B; RRID: AB_2661792
Anti-human CD56	Fluidigm	NCAM16.2, cat#3163007B; RRID: AB_2661813
Anti-human CD24	Fluidigm	ML5, cat#3166007B; RRID: AB_2661803
Anti-human CD16/32	ThermoFisher	93, cat#14-0161-82; RRID: AB_467133
Iridium	Fluidigm	cat#201192A
Anti-human CD1c	Biolegend	L161, cat#331522; RRID: AB_10720182
Anti-human CD116	Biolegend	4H1, cat#305902; RRID: AB_314568
Anti-human CD115	Biolegend	9-4D2-1E4, cat#347306; RRID: AB_2562441
Anti-mouse CD3	Biolegend	17A2, cat#100204; RRID: AB_312661
Anti-mouse CD19	Biolegend	6D5, cat#115506; RRID: AB_313641
Anti-mouse F4/80	Biolegend	BM8, cat#123116; RRID: AB_893481
Anti-mouse CD11c	Biolegend	N418, cat#117318; RRID: AB_493568
Anti-mouse CD115	R&D systems	460615, cat#FAB3818C; RRID: AB_1964651
Anti-mouse I-A/E-A	Biolegend	M5/114.15.2, cat#107639; RRID: AB_2565894
Anti-mouse CD26	Biolegend	H194-112, cat#137804; RRID: AB_2293047
Anti-mouse XCR1	Biolegend	ZET, cat#148218; RRID: AB_2565231
Anti-mouse CD172a	Biolegend	P84, cat#144022; RRID: AB_2650813
Anti-mouse CD16/32	Biolegend	93, cat#101321; RRID: AB_1877064
Anti-mouse IRF4	Biolegend	IRF4.3E4, cat#646405; RRID: AB_2563266

(*Continued on next page*)

Continued

REAGENT or RESOURCE	SOURCE	IDENTIFIER
Anti-mouse CCR7	Biolegend	4B12, cat#120110; RRID: AB_492841
X8 antibody labeling kit (tag-153Eu)	Fluidigm	cat#201153A
X8 antibody labeling kit (tag-173Yb)	Fluidigm	cat#201173A
Anti-APC antibody (tag-162Dy)	Fluidigm	APC003, cat#3162006B
Anti-GFP antibody (Alexa fluor488)	Biolegend	FM264G, cat#338007
M-CSF receptor antibody	Cell Signaling	cat#3152; RRID: AB_2085233
Phospho-M-CSF receptor (Tyr546) antibody	Cell Signaling	cat#3083; RRID: AB_1147674
Anti-mouse CSF1R antibody	Abcam	AFS98, cat#ab171226
Bacterial and Virus Strains		
Pseudomonas aeruginosa	ATCC	PAO1; RRID: SCR_006590
Biological Samples		
SBP-AG human BAL samples	University of Illinois at Chicago	UIC IRB No: 2009-0838
Chemicals, Peptides, and Recombinant Proteins		
Recombinant mouse CSF1	R&D systems	146-ML/CF
Recombinant mouse CSF2	R&D systems	415-ML/CF
Anti-CSF1 antibody (neutralizing)	R&D systems	MAB416; RRID: AB_2085088
Anti-CSF1 antibody (IHC)	Abcam	Ab99178; RRID: AB_11143555
Rat IgG2b isotype control	R&D systems	MAB0061; RRID: AB_357350
Tamoxifen	Sigmaaldrich	T5648
4-Hydroxytamosifen	Sigmaaldrich	H6278
Clodronate liposome	Clodronate liposome.org	http://www.clodronateliposomes.org
GW2580	Tocris	cat#5673
PLX647	Sigmaaldrich	Cat#SML0966
AP20187	Takara	Cat#635058
Critical Commercial Assays		
Human CSF1 (M-CSF) ELISA	R&D systems	DY216
Human CSF2 (GM-CSF) ELISA	R&D systems	DY215
Mouse IL-4 ELISA	R&D systems	DY404
Mouse IL-13 ELISA	R&D systems	DY413
Mouse IgE ELISA MAX Deluxe	Biolegend	cat#432405
CellTiter-Glo	Promega	cat#G7571
Experimental Models: Cell Lines		
Raw264.7	ATCC	ATCCTIB-71; RRID: CVCL_0493
Beas2b	ATCC	CRL-9609; RRID: CVCL_0168
Experimental Models: Organisms/Strains		
Mouse: C57BL/6	Jackson Laboratory	Stock No:000664; RRID: IMSR_JAX:000664
Mouse: B6N.129S6(Cg)-Scgb1a1tm1(cre/ERT)Blh/J (or Scgb1α1-iCre)	Jackson Laboratory	Stock No: 016225; RRID: IMSR_JAX:016225
Mouse: CSF1 floxed	Werner, SA lab	Harris et al., 2012
Mouse: C57BL/6-Tg(Csf1r-EGFP-NGFR/FKBP1A/TNFRSF6)2Bck/J (or MAFIA)	Jackson Laboratory	Stock No: 005070; RRID: IMSR_JAX:005070
Mouse: B6.129S1-Irf4tm1Rdf/J (or IRF4 floxed)	Jackson Laboratory	Stock No: 009380; RRID: IMSR_JAX:009380
Mouse: FVB-Tg(Csf1r-cre/Esr1*)1Jwp/J → Background changed to C57BL/6 by Christman, JW lab	Jackson Laboratory Christman Lab (Ohio University)	Stock No: 019098; RRID: IMSR_JAX:019098
Software and Algorithms		
viSNE	Cytobank	https://www.cytobank.org/
GraphPad prism	GraphPad software	https://www.graphpad.com/
FlowJo	TreeStar Inc	https://www.flowjo.com/

(*Continued on next page*)

Continued

REAGENT or RESOURCE	SOURCE	IDENTIFIER
Other		
Mouse dust mite: *D. pteronyssinus*	Greer lab	XPB82D3A25
Ragweed: *Ambrosia artermisiifolia*	Greer lab	XP56D3A25
Aspergillus fumigatus	Greer lab	XPM3D3A25

CONTACT FOR REAGENT AND RESOURCE SHARING

Further information and requests for resources and reagents should be directed to and will be fulfilled by the Lead Contact, Gye Young Park (parkgy@uic.edu).

EXPERIMENTAL MODEL AND SUBJECT DETAILS

SBP-AG Bronchoscopy Protocol

This protocol was approved by the Institutional Review Board of the University of Illinois (Chicago, IL) and an Investigational New Drug (IND) was obtained from the FDA for bronchoscopic administration of allergens to volunteers. The details of the protocol were described in our previous publication (Park et al., 2013). In brief, we recruited study subjects who are on step 1 asthma therapy according National Asthma Education and Prevention Program (NAEPP) Asthma Guidelines. After obtaining informed consent, subjects underwent screening for inclusion and exclusion criteria which included skin prick testing to dust mite, short ragweed and cockroach allergens. Once screening was complete, bronchoalveolar lavage (BAL) was performed per standard research guidelines approved by the IRB. Pre-challenge BAL samples were obtained right before sub-segmental broncho-provocation with the identified allergen (SBP-AG). At 48 hours after the SBP-AG, Post-challenge BAL samples were obtained. For the University of Wisconsin cohort, the protocol was approved by the University of Wisconsin Health Sciences Human Subjects Committee and informed written consent was obtained from all subjects. The mean age of the UIC and Wisconsin cohorts was 24 (range 18-36) and 25 (range 19-36) and the male to female ratios were 2:4 and 7:3 respectively.

Mice

C57BL/6, *Scgb1a1-cre*ERT (stock# 016225), *Irf4*$^{fl/fl}$ and MAFIA mice were purchased from Jackson Laboratory (Bar harbor, ME). Csf1fl/fl mice were described previously (Harris et al., 2012). *Csf1*$^{fl/fl}$ mice were cross-bred with *Scgb1a1-cre* to generate selective CSF1-deficient mice in airway epithelial cells. *Csf1r-cre*ERT mice were obtained from Dr. John Christman's lab at Ohio State University, Columbus, OH and crossbred with *Irf4*$^{fl/fl}$ to generate *Csf1r-cre*ERT;*Irf4*$^{fl/fl}$. Mice were bred in a specific pathogen-free facility maintained by University of Illinois at Chicago. All mice experiments were approved by the Institutional Animal Care and Use Committee of University of Illinois at Chicago. Mouse genotypes from tail biopsies were determined using real time PCR with specific probes designed for each gene (Transnetyx, Cordova, TN). Age & sex-matched 7 to 10-week-old mice were used for experiments.

Cell culture

All cells were purchased from ATCC (Manassas, VA) and cultured in RPMI 1640 and DMEM (Invitrogen) supplemented with 5% FBS & 1% penicillin and streptomycin for BEAS-2B cells and RAW 264.7 cells, respectively. BEAS-2B cells were cultured on transwell plates and stimulated by DRA for 24 hours. Supernatant was collected for ELISA. RAW 264.7 cells were pre-incubated with CSF1R inhibitors (1 μM) or DMSO vehicle for 1h and stimulated by recombinant CSF1 proteins for 20 min. Cells were collected for western blot.

METHOD DETAILS

DRA-induced asthma model and airway epithelial-specific CSF depletion

We used the previously described DRA-induced mouse asthma model with minor modification (Lee et al., 2015; Park et al., 2013). Both allergen sensitization and challenge were done through the intranasal route without adjuvant use. Tamoxifen (75 mg/kg, *i.p*; Sigma-Aldrich, St. Louis, MO) was injected for 5 consecutive days along with DRA sensitization on day 0, 2 and 4 (Madisen et al., 2010). All of the allergens were purchased from Greer Lab. (Lenoir, NC). Mice were challenged with DRA (*i.n.*) on day 10, 12, 14 and the BAL fluids and lung tissues were collected at designated time points. For recovery and neutralizing experiments, mouse recombinant CSF1 and anti-mouse CSF1 antibody (R&D systems, Minneapolis, MN) were administered along with DRA on day 10, 12 and 14. For the experiment with CSF1R inhibitors, GW2580 (Selleckchem, Houston, TX) were administered for 5 consecutive days during the allergen challenge period.

ZW800-conjuagted HDM

House dust mite (HDM) was conjugated with ZW800 as described previously (Moon et al., 2015). In brief, HDM was suspended in 1X PBS. Prepared ZW800-1C (Formula: $C_{51}H_{67}N_4O_8S_2^+$, MW: 928.23 Log D at pH 7.4: −2.80) (Choi et al., 2013) was added to HDM at a ratio of 1:1(v/v). The mixture was incubated for 4h at RT with rigorous shaking. ZW800-1C conjugated HDM was purified using P6 mini column and stored at −20°C until use (Choi et al., 2013).

P.aeruginosa lung infection

Mice under anesthesia were administered PBS or PA103 intratracheally at dose of 5×10^5 CFU/mouse suspended in 20μl of PBS. Mice were sacrificed by exsanguination under anesthesia. Tracheotomy was performed after 6 h, 12 h, and 24 h of PA injection with a 20-gauge intravenous catheter, which was tied into place. BAL was performed using 1 mL of room temperature PBS as described (Fu et al., 2013).

Western blot

Immunoblots were performed as described previously(Park et al., 2013) . Raw264.7 cells were pretreated for 1h with CSF1R inhibitors (each 1μM) and then stimulated with recombinant CSF1 (10 ng/ml) for 15 min. CSF1R and Phospho-CSF1R-Y546 antibodies were purchased from Cell Signaling Technologies (Danvers, MA).

ELISA

Human and mouse CSF-1 & CSF-2 ELISA kits were purchased from R&D systems (Minneapolis, MN), mouse IL-4, IL-13 from eBioscience (Waltham, MA) and IgE ELISA kit from BioLegend (San Diego, CA). All procedures followed by the manufacturer's instructions. For measuring DRA-reactive IgE, high affinity-binding 96-well plates were coated with the DRA allergens (D.f;100, ragweed;1000 and aspergillus;100 μg/ml, purchased from Greer Lab), in coating buffer for overnight at 4°C. Next, 1% bovine serum albumin (BSA) was used as blocking buffer for 1h at RT and the rest of the procedure followed the IgE ELISA kit protocol.

Histology, Immunohistochemistry (IHC) and immunofluorescent (IF) staining

Histologic tissue analyses were performed by Research Histology and Tissue Image Core (RHTIC) at UIC. Briefly, 4% paraformalin-fixed and paraffin-embedded sections of lung tissues were used for H&E, IHC and IF. Anti-CSF1 (Abcam, MA) and anti-Scgb1a1 (Santa Cruz Biotechnology, Santa Cruz, CA) were used and images were taken using an Olympus BX51 fluorescence microscope (Olympus). The Genie System (Aperio Technologies, Vista, CA) was used for automated quantification of tissue(lung) inflammation in whole slide images as described previously(Park et al., 2013).

Generation of BMDC and intratracheal adoptive transfer

To adoptively transfer dendritic cells and macrophages, we cultured BMDC and BMDM as described previously(Karpurapu et al., 2011). In adoptive transfer experiment with MAFIA mice, BMDC and BMDM were stimulated by HDM (10 μg/ml) for 3 hours. Before adoptive transfer, we depleted CSF1R positive cells in MAFIA mice by injecting AP20187 (1 mg/kg, *i.p*) as we published previously(Lee et al., 2015). DRA-pulsed BMDC ($1x10^5$cells/mouse) and BMDM ($1x10^5$ cells/mouse) were transferred via the intratracheal route. In adoptive transfer experiment, the donor $EGFP^+$ BMDC ($5 x10^5$cells/mouse) were cultured from MAFIA mice and transferred to the DRA-sensitized WT mice. Mice were challenged with DRA in the presence or absence of anti-CSF1 neutralizing antibody and then $EGFP^+$ cells were measured in mediastinal lymph node by flow cytometry. To study the effect of CSF1R inhibitor (GW2580) on *in vivo* migration of DCs, the recipient mice was treated with clodronate liposome (30 μl/mouse, *i.t*) to deplete intrinsic myeloid lineage cells. After then, the cultured $EGFR^+$ BMDC ($5 x10^5$cells/mouse) from MAFIA mice was transferred with or without the pretreatment of GW2580 at 1 hour prior to the adoptive transfer. Next, the challenge phase of the DRA model was done as described before (Figure 1C) and $EGFP^+$ cells were measured in the mediastinal lymph node of recipient mice by flow cytometry.

Ex vivo IgE production

Splenocytes were isolated from WT mice and cultured for overnight. The cells were treated with CSF1 (10 ng/ml) in the presence or absence of DRA (each 1, 10, 1 μg/ml) once or twice, as described in supplement Figure 5. The supernatants were collected and measured for total IgE by using ELISA.

Expression of CCR7 on cDCs

Single cells suspension was isolated from the whole lung tissue of WT mice and plated on 6-well plates for overnight. Next, the unattached cells were washed out with fresh 1XPBS and the adherent cells were stimulated with CSF1 (10 ng/ml) in the presence or absence of DRA (each 5, 50, 5 μg/ml) for 24h. After gating for cDC population as shown in Figure S5, the cells were measured for the expression of CSF1R and CCR7 by flow cytometry according to cDC1 and cDC2 population, respectively. To study the effect of CSF1R inhibitor on CCR7 expression, GW2580 (0.1 and 1μM) was given 1 hours prior to CSF1 stimulation with or without DRA.

FACS analysis

BAL cells and mediastinal lymph nodes were prepared as described previously (Moon et al., 2010). Anti-CD26 (PE), anti-CD11c (PE-Cy7), anti-F4/80 (APC), anti-CD172a (AF700), anti-XCR1 (BV480) and anti-I-A/I-E (BV610) were purchased from BioLegend

and anti-CSF1R (Percp) from R&D systems. Samples were run through a Gallios flow cytometer (Beckman Coulter, Pasadena, CA) and analyzed by Flowjo software (FlowJo, LLC, Ashland, OR). A complete listing of the antibodies used for this study is available in the Supplementary online data.

Mass Cytometry Analysis

Human BAL cells were obtained from pre- and post-allergen challenged BAL fluids. Each $3x10^6$ cells were used for staining and followed manufacturer's instruction (Becher et al., 2014). In brief, cells were resuspended in Maxpar Cell Staining Buffer and added Fc-receptor blocking solution for 10 min at RT. Antibody cocktail was added and incubated for 30 min. at RT. After washing, cell intercalation solution was added and incubated for 1 hour at RT and then washed with Maxpar Water. Cells were run by Helios™ and analyzed by viSNE from Cytobank (Santa Clara, CA). Metal-conjugated antibodies were purchased from Fluidigm (South San Francisco, CA) and are listed in the supplementary online data.

Surface Plasmon Resonance (SPR) binding analysis

The binding analyses were performed on a Biacore T200 instrument (GE Healthcare) according to the manufacturer's instructions. The CSF1R (SignalChem) was purchased and buffer exchanged using Zeba™ Spin desalting columns (Thermo Scientific) to remove Tris. The CSF1R was diluted with 10 mM sodium acetate (pH 4.0) and immobilized to flow channels 2 and 4 on a Series S sensor chip CM5 (GE Healthcare) using standard amine coupling method with running buffer HBSP (10 mM HEPES, 150 mM NaCl, 0.05% surfactant P-20, 1mM ZnCl2, pH 7.4). Two unmodified surfaces on flow channels 1 and 3 were used as controls. Three testing compounds (PLX647, GW2580 and a negative control compound) were initially prepared as 10 mM stocks in 100% DMSO solutions. Compound solutions with a series of increasing concentrations (0 – 40 μM at 2-fold dilution) were applied to all four channels in SPR binding buffer (HBSP + 0.5 mM TCEP + 2% DMSO) at a 30 μL/min flow rate at 25°C. Sensorgrams were double-referenced with blank channel and zero concentration signals, and analyzed using the Biacore T200 evaluation software v3.0. Sensorgrams were best fit with a two-state binding model that is described by the following equation:

$$A + B \underset{k_{d1}}{\overset{k_{a1}}{\rightleftarrows}} AB \underset{k_{d2}}{\overset{k_{a2}}{\rightleftarrows}} AB^*$$

where $K_A = (k_{a1}/k_{d1})(1+k_{a2}/k_{d2})$ and $K_D = 1/K_A$. In the two-state binding model, molecules A (ligand; CSF1R) and B (analyte; compound) bind into an initial complex AB, and then undergoes a conformational change and makes a stable AB* complex. The K_D values were calculated from association rate (k_a) and dissociate rate (k_d) constants.

QUANTIFICATION AND STATISTICAL ANALYSIS

Two-sample t test was used for two group comparisons and ANOVA was used for comparing multiple groups. To analyze paired samples, the paired t test was used. Unless specifically denoted in the Figures, $^*p < 0.05$ or $^{**}p < 0.01$ were considered statistically significant. The tests were two-sided and all our data met the assumptions of the test. Data are presented as mean ± SEM. No statistical methods were used to predetermine sample sizes, but our distribution was assumed to be normal and variances were assumed to be equal across groups, but this was not formally tested. All analyses were conducted using Prism, GraphPad Software (La Jolla, CA).